Transactive Control of Commercial Buildings for Demand Response

He Hao, Charles D. Corbin, Karanjit Kalsi, and Robert G. Pratt

***Abstract*—Transactive control is a type of distributed control strategy that uses market mechanisms to engage self-interested responsive loads to achieve power balance in the electrical power grid. In this paper, we propose a transactive control approach of commercial building heating, ventilation, and air-conditioning (HVAC) systems for demand response. We first describe the system models, and identify their model parameters using data collected from systems engineering building (SEB) located on our Pacific Northwest National Laboratory campus. We next present a transactive control market structure for commercial building HVAC systems, and describe its agent bidding and market clearing strategies. Several case studies are performed in a simulation environment using building controls virtual test bed (BCVTB) and calibrated SEB EnergyPlus model. We show that the proposed transactive control approach is very effective at peak shaving, load shifting, and strategic conservation for commercial building HVAC systems.**

***Index Terms*—Commercial buildings, demand response, HVAC systems, market mechanism, transactive control.**

I. Introduction

DEMAND response (DR) is defined as "Changes in electric usage by end-use customers from their normal consumption patterns in response to changes in the price of electricity over time, or to incentive payments designed to induce lower electricity use at times of high wholesale market prices or when system reliability is jeopardized" [1]. Among various demand-side resources, commercial buildings consume about 36% of the total electricity in the United States. In particular, there are about 5.6 million commercial buildings, comprising 87.4 billion square feet of floorspace and contributing to $1/3$ of peak demand [2], [3]. The massive power consumption and enormous thermal storage capability of commercial buildings make them great resource for DR [4]–[8].

DR strategies can be generally classified into three types: 1) price-based; 2) direct load control (DLC); and 3) transaction-based. Price-based DR relies on customers changing their electricity consumption in response to time-varying pricing mechanisms such as time-of-use, critical peak, and real-time pricings [9]. It is simple and easy to deploy but its challenge is reliability and predictability. The unpredictable quantity and quality has created a barrier for accurate DR [10]. Moreover, large scale DR programs under the real-time pricing scheme will create volatility for the power system, and present more challenges for maintaining the stability of the grid [11]. DLC allows utilities or system operators to remotely control (e.g., turn on and off) specific electric loads in paticipants' premise during peak demand periods and critical events [12], [13]. The main advantage of DLC is that the operator has more certainty about the amount of load being shifted [14]. However, DLC involves direct communication with individual appliances or loads. It might not strictly respect customer's privacy and preferences, but recent work showed that certain incentive-based contracts could enable DLC with preference revealing [15].

Transactive control, sometimes called market-based control, is a distributed control strategy that uses market mechanisms to engage self-interested responsive loads to provide services to the grid. The only information needing to be exchanged between the electric loads and system operator are the price and quantity of desired electricity consumption, and therefore it respects customers' privacy, preference, and freewill. We comment that different DR strategies are suitable for different applications depending on the nature and requirements of the provided services. It is believed that for a grid service that is at a time resolution shorter than five minutes (such as frequency regulation), DLC is more appropriate to ensure the reliability and certainty of the program [14], [16]. For planning services that are at larger time scales (from months to years), certain contract-based mechanisms will be sufficient. It is to our view that, transaction-based DR is more appropriate for grid services that are at time scales from minutes to hours.

Aggregation and coordination of residential loads for DR has recently received a lot of attention, and various modeling and control strategies have been proposed. For example, a couple of novel pricing methods were proposed in [17], [18] to coordinate residential loads and electric vehicles for grid services. In [19], [20], the authors studied aggregation and control of residential thermostatically controlled loads to manage power and energy imbalance. Markov decision process and mean-filed game were used to control residential pool pumps for ancillary services [21], [22]. In [23], [24], market-based distributed coordination mechanisms of various types of residential loads were developed. Characterizing the flexibility of residential loads for regulation service and renewable integration have been studied in [25], [26].

In this paper, we focus on control of commercial building heating, ventilation, and air-conditioning (HVAC) system for DR. There are several closely-related work on transactive control of building HVAC systems. A reference guide of a transaction-based building control framework was presented

Manuscript received December 8, 2015; revised March 15, 2016; accepted April 19, 2016. Date of publication April 27, 2016; date of current version December 20, 2016. Paper no. TPWRS-01757-2015.

The authors are with the Electricity Infrastructure and Buildings Division of Pacific Northwest National Laboratory, Richland, WA 99354 USA (e-mail: He.Hao@pnnl.gov; Charles.Corbin@pnnl.gov; Karanjit.Kalsi@pnnl.gov; Robert.Pratt@pnnl.gov).

Color versions of one or more of the figures in this paper are available online at http://ieeexplore.ieee.org.

Digital Object Identifier 10.1109/TPWRS.2016.2559485

in [27]. In [28], [29], transactive control of residential HVAC systems has been demonstrated in the Olympic Peninsula and American Electric Power (Ohio) projects. Similar ideas as those in [28], [29] were applied to control of thermostats in commercial building HVAC systems in [30]. However, the work in [30] only considered a single-auction market, in which thermostats were purely reactive to an external price signal. The thermostats did not bid a "quantity" of commodity into a market, and they simply used the price signal to adjust their temperature set points. Another related work on transactive market mechanism design is [31]. However, [31] considered residential HVAC systems, whose dynamics are simpler, and there were only one market and two hierarchies: residential air conditioners and distribution system operator. A double-auction market-based control approach for a commercial HVAC system was implemented in [32], where the goal was to distribute the amount of airflow fairly to each zone. Nonetheless, the research in [32] only focused on the distribution of airflow, and didn't consider the interactions among variable air volume (VAV) boxes, air handling unit (AHU), chiller, and other components in the HVAC system for DR.

To fully unlock the potential of commercial buildings for DR, it is essential to engage various components in the HVAC system to collectively achieve this objective. In this paper, we propose a novel transactive control approach to fully engage various HVAC subsystems, and develop a double-auction market structure and mechanism to coordinate them for DR. Compared with previous research [28]–[32], the main contributions of our paper are, we consider commercial HVAC systems, whose dynamics have nontrivial non-linearity, and multiple heterogeneous agents, markets and hierarchies in the market mechanism. Additionally, we characterize the power flexibility of the HVAC system that can be offered to the grid, subject to temperature and/or operational constraints of each HVAC component. Our approach is able to provide reliable and accurate DR to the grid while respecting the comfort and preference of the occupancy.

Furthermore, we present various thermal and power models for the HVAC components, and use measurement data collected from the newly-constructed systems engineering building (SEB) to identify their model parameters. We show that predictions using our models and identified parameters fit extremely well with the measurement data. Moreover, we set up a simulation environment using the building controls virtual test bed (BCVTB) [33], and EnergyPlus [34]. The designed transactive control strategies are implemented using Python in the BCVTB, and the EnergyPlus model is calibrated using measurement data from the SEB. We show that the proposed transactive market mechanism is very effective at peak shaving, load shifting, and strategic conservation, while having little impact on the building indoor temperature.

The rest of the paper is organized as follows. In Section II, we present HVAC system modeling and identification. A transactive market structure and mechanism for commercial building HVAC system is proposed in Section III. Section IV is devoted to experiment setup and numerical simulations. The paper ends with conclusions and future work in Section V.

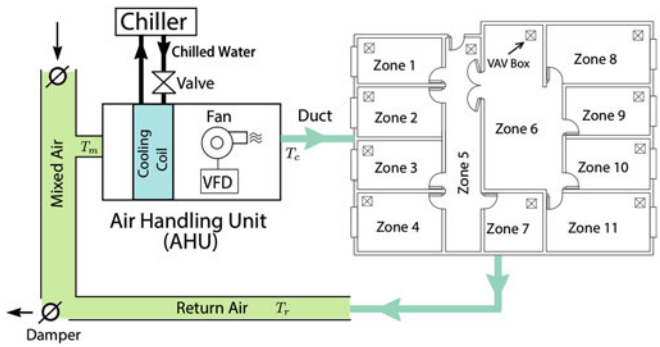

Fig. 1. Configuration of a typical commercial building HVAC system [6].

II. System Modeling and Identification

A. Zone Thermal Model

A typical configuration of a multi-zone commercial building HVAC system includes AHU, chiller, and VAV boxes, as shown in Fig. 1. A detailed description of these main components and their functionality can be found in [6], [35].

We consider a commercial HVAC system with n zones. For each temperature zone $i = 1, \ldots, n$, there is a VAV box associated with it, and we use the following simple model to describe its temperature evolution [4], [36],

$$C^i \frac{dT^i(t)}{dt} = \frac{T_o(t) - T^i(t)}{R^i} + q^i(t) + q_x^i(t), \tag{1}$$

where $T^i(t)$ is zone temperature, C^i, R^i are respectively its thermal capacitance and thermal resistance, $T_o(t)$ is the outside temperature, and $q_x^i(t)$ is the external disturbances from solar, occupancy, and appliances, etc. Moreover, $q^i(t) = -q_c^i(t) + q_h^i(t)$, where $q_c^i(t)$ is the cooling power provided by the cooling coil, and q_h^i(t) is the reheating power from the VAV box,

$$q_c^i(t) = c_a \dot{m}^i(t)(T^i(t) - T_c(t)),$$
$$q_h^i(t) = c_a \dot{m}^i(t)(T_s^i(t) - T_c(t)),$$

in which c_a is the specific heat of air, $\dot{m}^i(t)$ is the supply airflow rate, $T_c(t)$ is the discharge air temperature, and $T_s^i(t)$ is the supply air temperature.

In this paper, we approximate the zone thermal dynamics (1) by a linear model of the form,

$$T_{t+1}^i = a_1^i T_t^i + a_2^i T_{o,t} + a_3^i q_{t+1}^i + a_4^i q_t^i + a_5^i, \tag{2}$$

where coefficients a_1^i, a_2^i, a_3^i, a_4^i, and a_5^i can be found through linear regression, and t is the current time index. In this model, q_{t+1}^i and T_{t+1}^i represent the cooling rate and temperature measured at the next time index, and $a_4^i q_t^i + a_5^i$ provides an estimate of the unobserved external disturbances as measured by the cooling rate at the current time, q_t^i. We may also rearrange (2) to find coefficients for predicting q_{t+1}^i given desired future temperature, T_{t+1}^i. Section II-D provides model justification and calibration of model (2).

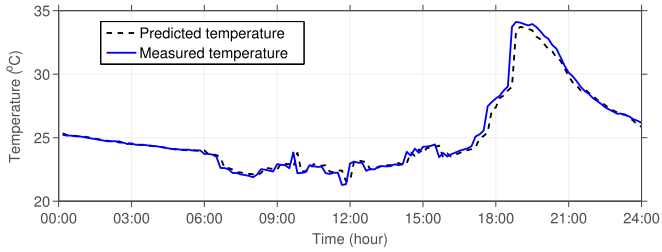

Fig. 2. Comparison between measured and predicted temperatures.

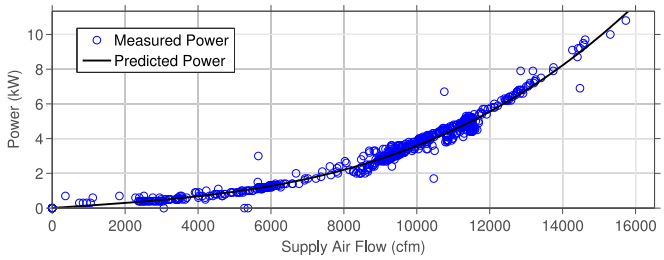

Fig. 3. Comparison between measured and predicted fan powers.

B. Supply Fan Model

The total airflow supplied by the fan is equal to the summation of the supply airflow into each individual zone

$$\dot{m}_t = \sum_{i=1}^{n} \dot{m}_t^i.$$

We model the fan power as a polynomial function of the total airflow [35], [37], [38]

$$q_t^f(\dot{m}_t) = b_1(\dot{m}_t)^3 + b_2(\dot{m}_t)^2 + b_3\dot{m}_t + b_4, \qquad (3)$$

where b_1, b_2, b_3 and b_4 are constants that will be identified using the least squares method.

C. Chiller Model

Several detailed complex chiller models have been presented in literature, e.g., [38]–[41]. However, these models are very complex, and not amenable to control applications. In this paper, we consider a simple control-oriented chiller model [35], [36],

$$q_t^c = \frac{c_a\dot{m}_t(T_m - T_c)}{\eta \text{COP}},$$

where $T_m = \delta\frac{\sum_i \dot{m}_t^i T_t^i}{\sum_i \dot{m}_t^i} + (1-\delta)T_o$ is the mixed air temperature, $\delta \in [0,1]$ is the damper position, η is the efficiency factor of the cooling coil, and COP is the Coefficient of Performance of the chiller. The chiller power model can be rewritten as

$$q_t^c = \delta\frac{\sum_{i=1}^n q_{c,t}^i}{\eta \text{COP}} + (1-\delta)\frac{c_a\dot{m}_t(T_{o,t} - T_c)}{\eta \text{COP}}.$$

D. System Identification Using SEB Measurement Data

We regress data measured from the SEB to find model coefficients for (2) using R programming language and software environment [42]. The identified model parameters for one of the 17 zones are given by $a_1^1 = 0.9593, a_2^1 = 0.0109, a_3^1 = -1.177 \times 10^{-3}, a_4^1 = 9.397 \times 10^{-4}$, and $a_5^1 = 0.8166$. We observe that for all coefficients, $|P| \ll 0.05$. Fig. 2 depicts the comparison between the measured temperature and the predicted temperature using model (2) and identified model parameters. We see that they match each other very well. Identified fan power parameters are $b_1 = 2.569 \times 10^{-12}, b_1 = -4.451 \times 10^{-9}, b_3 = 1.459 \times 10^{-4}$, and $b_4 = 4.711 \times 10^{-3}$, and the R-squared is 0.9868. Fig. 3 depicts the comparison between measured fan power and predicted fan power using (3) and identified fan model parameters. Again, we observe that the predicted fan power is a good approximation of the measured fan power.

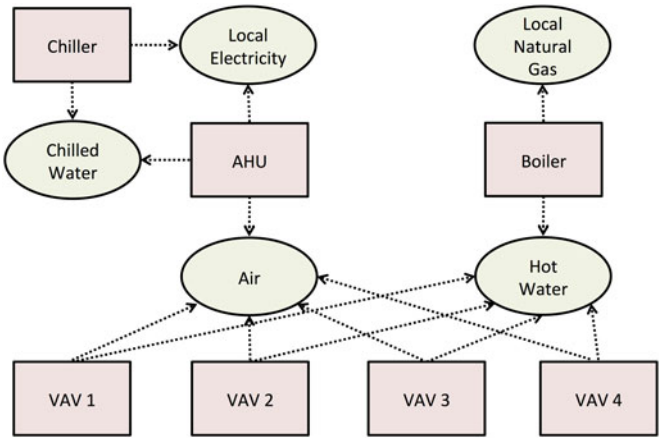

Fig. 4. Transactive market structure for commercial building HVAC systems.

Moreover, we calculate an average efficiency factor $\eta = 0.8879$ for the cooling coil, and an average COP $= 5.9153$ for the chiller.

III. Transactive Market Structure and Mechanism

A. Transactive Market Structure

In this section, we present a *virtual* market structure for commercial building HVAC systems. We comment that the main purpose of this virtual market structure is to design a distributed transactive control strategy. It does not represent a real energy market with financial transactions. In this market structure (depicted in Fig. 4), there are five markets (represented in ovals): 1) conditioned air market, 2) chilled water market, 3) local electricity market, 4) hot water market, and 5) local natural gas market, and there are six types of agents (represented by rectangles): 1) VAV boxes, 2) AHU, 3) chiller, 4) boiler, 5) local electricity provider (not shown), and 6) local natural gas provider (not shown). Arrows indicate direction of bids. Markets are cleared every Δt minutes, and the quantity of commodity in each market is expressed in terms of kWh.

If all zones require cooling and no reheating is required (i.e., $q^i = -q_c^i$ for all i), the hot water and local natural gas markets are disabled. In this case, we only need to consider the conditioned air, chilled water, and local electricity markets. On the other hand, if all zones require reheating, then the airflow of each zone is set to its minimum value. In this case, there is little flexibility from the "electricity" side, since the total airflow (and thus fan power) and the required amount of chilled water (and thus chiller power) are fixed. In practice, some zones require

cooling, and the others require reheating. Since we are interested in exploiting the power flexibility of HVAC system for DR to the grid, we only consider the zones that require cooling, and treat the zones require reheating as passive (uncontrollable) loads.

The information flow, market bidding and clearing process are described as follows. First, based on the thermal requirement of a zone, each VAV box submits a demand curve for conditioned air into the air market. After collecting all bids from the VAV boxes, the AHU constructs an aggregate demand curve for the air market. From this aggregate demand curve, the AHU constructs chilled water and electricity demand curves, and bids them into the chilled water and local electricity markets. Next, the chiller constructs an electricity demand curve from the chilled water demand curve submitted by the AHU, and submits it to the local electricity market. In the local electricity market, an aggregate demand curve is constructed using curves submitted by the chiller and AHU. The local electricity market clears at the intersection of this demand curve and a supply curve submitted by a local electricity provider. The point of intersection determines the market clearing price (MCP) of electricity and traded capacity. The chilled water and conditioned air markets then clear. The MCP of air is then passed down to the VAV boxes, and each VAV box determines its energy consumption based on the MCP and its own demand curve. Each zone then calculates its temperature setpoint at the next time step using (2). At the next time step, all agents receive updated system states and external information (e.g., outside temperature), and repeat the market process until the end of the considered time horizon.

B. Transactive Market Mechanism

We next present a transactive market mechanism to form a theoretical basis for the above market structure. In the HVAC system, each VAV box (indexed by i) is modeled as a self-interested agent, who needs to determine the amount of air to consume to maximize its own utility function

$$U^i = V^i(Q^i) - p^a Q^i,$$

where $Q^i = q^i \Delta t$ is the amount of air it desires, $V^i(Q^i)$ is its value function representing the satisfaction of consuming Q^i amount of air, and p^a is the price of air. Moreover, we assume V^i is continuously differentiable and strongly concave. The utility maximization problem for each zone i is formulated as

$$\text{maximize } V^i(Q^i) - p^a Q^i \tag{4a}$$

$$\text{subject to: } Q^i_- \le Q^i \le Q^i_+, \tag{4b}$$

where Q^i_- and Q^i_+ are respectively its minimum and maximum conditioned air requirements.

The AHU's utility function is defined as its revenue minus cost

$$U^{\mathrm{A}} = p^a \sum_i Q^i - p^e Q^f - p^w Q^w,$$

where p^e, p^w are respectively the prices of electricity and chilled water, and Q^f, Q^w are respectively the desired amounts of electricity and chilled water requested by the AHU's fan and cooling coil. Similarly, the chiller's utility function is

$$U^{\mathrm{C}} = p^w Q^w - p^e Q^c,$$

where Q^c is the desired amount of electricity by the chiller. Moreover, in the local electricity market, there is a cost $C(Q^f + Q^c)$ incurred by providing Q^f amount of electricity to the supply fan and Q^c amount of electricity to the chiller. In this paper, we assume $C(Q)$ is differentiable and nondecreasing in Q. The local electricity provider's utility function is given by

$$U^{\mathrm{P}} = p^e(Q^f + Q^c) - C(Q^f + Q^c).$$

We assume the transactive market is a competitive market managed by a nonprofit entity such as the building manager. The social welfare is defined as the summation of the utility functions of the electricity provider, chiller, AHU, and VAV boxes [43]. Plugging into expressions for the utility functions, we get the following formula for the social welfare

$$\text{Social Welfare} = \sum_{i=1}^n V^i(Q^i) - C\Big(Q^f + Q^c\Big).$$

The social welfare maximization (SWM) problem is formulated as the following convex optimization problem

$$\text{maximize } \sum_{i=1}^n V^i(Q^i) - C\big(g(Q^1, \cdots, Q^n)\big) \tag{5a}$$

$$\text{subject to: } g\big(Q^1, \cdots, Q^n\big) - D \le 0, \tag{5b}$$

$$Q^i_- \le Q^i \le Q^i_+, \quad \forall\, i = 1, \ldots, n, \tag{5c}$$

where $D/\Delta t$ is the peak demand limit of the commercial building HVAC system, and $g(Q^1, \cdots, Q^n) : \mathcal{R}^n \to \mathcal{R}$ is the electrical energy consumption of the HVAC system,

$$g(Q^1, \cdots, Q^n) = q^f\Big(\sum_i \frac{Q^i/\Delta t}{c_a(T^i - T_c)}\Big)\Delta t + \delta\frac{\sum_{i=1}^n Q^i}{\eta \mathrm{COP}} + (1-\delta)\frac{(T_o - T_c)\sum_{i=1}^n Q^i/(T^i - T_c)}{\eta \mathrm{COP}}$$

in which $q^f(\cdot)$ is given by (3).

In practice, each VAV box's value function, $V^i(\cdot)$, may be private, in which case it is impossible for a coordinator (e.g., a building manager) to solicit this information and solve the SWM problem in a centralized way. Therefore, the coordinator needs to set the conditioned air price $(p_a^{1,*}, \cdots, p_a^{n,*})$ so that the optimal solution of (4), $(Q^{1,*}, \cdots, Q^{n,*})$, also maximizes the social welfare. The following theorem shows that there exist unique optimal conditioned air prices and an optimal solution. Its proof is given in the Appendix.

Theorem 1. There exist optimal conditioned air price $(p_a^{1,*}, \cdots, p_a^{n,*})$ and optimal solution $(Q^{1,*}, \cdots, Q^{n,*})$ that maximize both the individual utility (4) and the social welfare (5). In particular, the optimal conditioned air price is given by $p_a^{i,*} = \max\{\nabla C(Q^*), \bar{P}\}\nabla g_i(Q^{1,*}, \cdots, Q^{n,*})$, where $\nabla C(Q^*)$ is the derivative of C at Q^*, $\bar{P}$ is the price determined by evaluating the aggregate demand curve in the local electricity market at the quantity of D, and ∇g_i is the partial derivative of g with respect to the i^{th} variable.

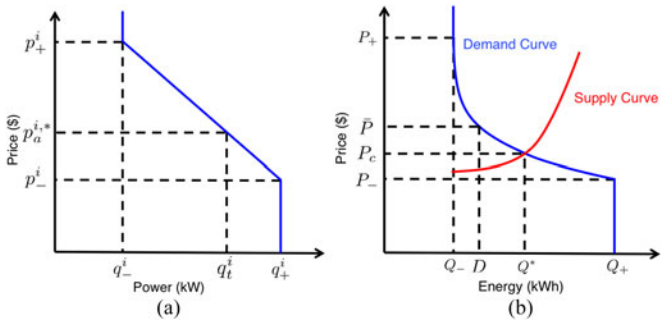

Fig. 5. Schematic demonstration of market clearing. (a) Zone demand curve. (b) Local electricity market.

C. Agent Bidding Strategies

In practice, the value function $V^i(\cdot)$ is very abstract, and it may be difficult for the occupants to quantity. To resolve this problem, we design bidding strategies for each VAV box to express their preferences and to implement the above transactive market mechanism.

To proceed further, we first show the connection between the optimality conditions of the SWM problem and the market clearing mechanism determined by the intersection of supply and demand curves. The first-order optimality condition of the SWM problem requires for each $i = 1, \cdots, n$,

$$\nabla V^i(Q^{i,*}) + \nu_1^{i,*} - \nu_2^{i,*} - \lambda^*(g(Q^{1,*}, \cdots, Q^{n,*}) - D) - (\lambda^* + \nabla C(Q^*))\nabla g_i(Q^{1,*}, \cdots, Q^{n,*}) = 0.$$

In particular, $\nabla C(\cdot)$ represents the marginal cost of electricity production, $\nabla V^i(\cdot)$ denotes the marginal benefit of consuming conditioned air, and $\nabla g_i(\cdot)$ is a scaling factor that transforms electricity price to conditioned air price. More precisely, $\nabla C(\cdot)$ is the electricity provider's supply curve, and $\nabla V^i(\cdot)$ is the VAV box's demand curve. Furthermore, it can be shown that the KKT optimality condition is equivalent to the interpretation of Fig. 5(b). For example, in the case of no constraint being binding, we have

$$\nabla C(Q^*) = \nabla V^i(Q^{i,*}) / \nabla g_i(Q^{1,*}, \cdots, Q^{n,*}).$$

This means that for each VAV box, the marginal benefit at $Q^{i,*}$ scaled by $\nabla g_i(Q^{1,*}, \cdots, Q^{n,*})$ is equal to marginal cost of electricity. Moreover, because $Q^* = Q^{f,*} + Q^{c,*} = g(Q^{1,*}, \cdots, Q^{n,*})$, this implies that in the electricity market the supply curve intersects with the aggregate demand curve, which is obtained by horizontally summing the demand curves of the AHU and chiller. Additionally, if only the peak demand constant is binding, i.e., $g(Q^1, \cdots, Q^n) = D$, we have

$$(\lambda^* + \nabla C(Q^*)) = \nabla V^i(Q^{i,*}) / \nabla g_i(Q^{1,*}, \cdots, Q^{n,*}),$$

where $\bar{P} = \lambda^* + \nabla C(Q^*)$ is the price determined by evaluating the demand curve at quantity D. Moreover, if $\nu_1^{i,*}$ or $\nu_2^{i,*}$ is positive, then $Q^{i,*} = Q_-^i$ or $Q^{i,*} = Q_+^i$. In this case, we have

$$\max\{\nabla C(Q^*), \bar{P}\} = \frac{\nabla V^i(Q^{i,*}) + \nu_1^{i,*}}{\nabla g_i(Q^{1,*}, \cdots, Q^{n,*})},$$

or

$$\max\{\nabla C(Q^*), \bar{P}\} = \frac{\nabla V^i(Q^{i,*}) - \nu_2^{i,*}}{\nabla g_i(Q^{1,*}, \cdots, Q^{n,*})}.$$

This implies that the optimal conditioned air price is higher than the maximum price p_+^i or lower than the minimum price p_-^i of the i^{th} VAV box's demand curve (see Fig. 5(b)).

We first design the demand curve for the VAV boxes.

a) VAV boxes: To construct a demand curve, each VAV box determines its minimum and maximum cooling power requirements q_-^i and q_+^i. Mathematically,

$$q_-^i = \max\left\{c_a \dot{m}_-^i (T_t^i - T_c), \frac{T_+^i - a_1^i T_t^i - a_2^i T_{o,t} - a_4^i q_t^i - a_5^i}{a_3^i}\right\},$$

$$q_+^i = \min\left\{c_a \dot{m}_+^i (T_t^i - T_c), \frac{T_-^i - a_1^i T_t^i - a_2^i T_{o,t} - a_4^i q_t^i - a_5^i}{a_3^i}\right\},$$

where T_-^i, T_+^i are the minimum and maximum temperature limits of zone i, $\dot{m}_-^i, \dot{m}_+^i$ are its minimum and maximum airflow limits, and T_c is the discharge air temperature which is usually fixed at 12.5^oC. In this paper, we design the bidding price in Fig. 5(a) as

$$p_-^i = \frac{P_a - k^i \sigma}{\eta \text{COP}}, \quad p_+^i = \frac{P_a + k^i \sigma}{\eta \text{COP}},$$

where P_a is the average electricity price over a certain period, σ is the standard deviation of the electricity price over the same period, and k^i is a user-specified tradeoff parameter that balances energy efficiency and comfort [29], [31].

b) AHU: After collecting the demand curves from all VAV boxes and their current zone temperatures, T_t^i's, the AHU determines the total supply airflow rate $\dot{m}_t = \sum_i \dot{m}_t^i = \sum_i \frac{q_t^i}{c_a(T_t^i - T_c)}$, the amount of required electricity by the supply fan $Q^f = q^f \Delta t$, and the amount of required chilled water $Q^w = \delta \frac{\sum_i q_t^i}{\eta} \Delta t + (1-\delta)\frac{c_a \dot{m}(T_o - T_c)}{\eta} \Delta t$. Based on the minimum and maximum cooling power requirements of all zones, the minimum and maximum amount of electricity the AHU bids into the local electricity market is given by

$$Q_-^f = q^f(\dot{m}_-)\Delta t, \quad Q_+^f = q^f(\dot{m}_+)\Delta t,$$

where the minimum and maximum fan power $q^f(\dot{m}_-), q^f(\dot{m}_+)$ are determined by (3) which are functions of the minimum and maximum airflow rates $\dot{m}_- = \sum_i \frac{q_-^i}{c_a(T_t^i - T_c)}, \dot{m}_+ = \sum_i \frac{q_+^i}{c_a(T_t^i - T_c)}$. Additionally, the minimum and maximum amounts of chilled water the AHU bids into the chilled water market are given by

$$Q_-^w = \delta\left(\frac{\sum_i q_-^i}{\eta}\right)\Delta t + (1-\delta)\left(\frac{c_a \dot{m}_-(T_o - T_c)}{\eta}\right)\Delta t,$$

$$Q_+^w = \delta\left(\frac{\sum_i q_+^i}{\eta}\right)\Delta t + (1-\delta)\left(\frac{c_a \dot{m}_+(T_o - T_c)}{\eta}\right)\Delta t.$$

Moreover, the bidding prices of the electricity and chilled water demand curves are determined by the aggregate demand curve from the VAV boxes.

c) Chiller: The chiller constructs an electricity demand curve from the chilled water demand curve submitted by the AHU. Specifically, the electrical power the chiller consumes is given by $Q_t^c = \frac{Q_t^w}{\text{COP}}$, and the minimum and maximum electrical power in the demand curve are given by

$$Q_-^c = \frac{Q_-^w}{\text{COP}}, \quad Q_+^c = \frac{Q_+^w}{\text{COP}}.$$

In addition, the bidding prices are uniquely determined by the demand curve submitted by the AHU.

The power flexibility of the commercial building HVAC system is then given by $\mathcal{F} = [Q_-/\Delta t, Q_+/\Delta t]$, where

$$Q_- = Q_-^f + Q_-^c, \quad Q_+ = Q_+^f + Q_+^c.$$

The power flexibility $\mathcal{F}$ represents the building's DR capability at the current period, e.g., the amount of power can be shaved. Given any power dispatch $Q/\Delta t \in \mathcal{F}$, it can guarantee the HVAC system is able to track $Q/\Delta t$, while ensuring each zone's thermal requirement is strictly satisfied.

Remark 1. There are many different bidding strategies that have been studied in literature. For instance, supply function equilibrium and residual demand derivative strategies considering transmission constraints in power system were studied in [44], [45]. DR with capacity constrained supply function bidding was investigated in [46]. A parameterized supply function bidding strategy was considered in [47]. A detailed review of bidding strategies is beyond the scope of this paper. Additionally, there are also many different coordination mechanisms to engage responsive loads for DR. It is to our view that they are complementary to each other, and there are some trade-offs among different approaches. For example, there are some trade-offs between our approach (which is similar to that in [28], [29], [31]) and the method in [23], [24] in terms of algorithm convergence rate and the amount of exchanged information. On the one hand, the algorithm in [23], [24] involves iterative interaction between responsive loads and a coordinator. It takes multiple iterations to reach the optimal solution, but the only information exchanged in each iteration are a single value of price and a single value of desired amount of electricity. On the other hand, our approach is able to find the optimal price in one shot, but each agent has to bid a demand curve, which expresses the consumer's desired amount of commodity at different prices.

IV. Experiment Setup and Simulation Results

A. Experiment Setup

Our co-simulation environment combines the BCVTB, EnergyPlus, and a Python implementation of the market and system models described previously. The EnergyPlus model is constructed from as-built drawings of the SEB and calibrated using measurement data from the building automation system. In our experiment, we only consider AHU 1 which serves 17 thermal zones. We select a hot summer week from the Pasco, WA typical meteorological year (TMY3) weather file for our simulations, and assume all considered zones are in cooling mode. This assumption reduces the transactive market structure in Fig. 4 to a conditioned air market in which zone agents transact with the AHU agent, a chilled water market in which the AHU agent buys chilled water from the chiller, and a local electricity market in which the AHU and chiller agents purchase electricity from a local electricity provider.

In our simulations, time is discretized with a 5-minute step size, and markets clear every 5 minutes. The simulations proceed as follows: (1) EnergyPlus simulates the first time step and the BCVTB transfers current zone temperatures, supplied HVAC cooling, and outside temperature, etc. to the Python implementation; (2) Agents in the Python implementation representing zones, AHU, and chiller construct demand curves and bid them correspondingly into the conditioned air, chilled water, and local electricity markets; (3) The electricity market first clears using one of the three different incentive signals (see Sections IV-B, IV-C, and IV-D). Chilled water and conditioned air markets then clear; (4) The cleared conditioned air price is then communicated to zones, which update their temperature set points. The Python implementation then sends the set points to EnergyPlus via the BCVTB. The process repeats for the next time step.

We conduct the following simulations: peak load shaving (see Section IV-B), responding to a real-time-price (RTP) signal (see Section IV-C), and strategic energy conservation (see Section IV-D). In the simulations, we assume thermal zones have temperature flexibility between 19 °C and 23 °C, and a simulation with constant 21 °C temperature set point is used as a baseline.

B. Simulation: Peak Load Shaving

This experiment tests the ability of the transactive market mechanism to cap building HVAC power under a peak demand limit, D. The peak demand limit is taken as 10.9 kW, or about 10% less than the peak demand of the baseline. Moreover, it is within the characterized power flexibility of the HVAC system, and the market clearing mechanism guarantees that this demand will not be exceeded while respecting zone temperature constraints. In this experiment, upper and lower prices bid by zones are set at $\$100$ and $\$10$, respectively. When predicted demand is lower than the peak demand limit D, the thermostats default to their nominal set point of 21 °C. When predicted demand is higher than the peak demand limit D, the electricity market clears at a price that is determined by the intersection of the demand curve and a vertical line passing the point $(D, 0)$, as illustrated in Fig. 5(b). Fig. 6 shows the HVAC power consumption and zone temperatures for the second day of the simulated week, when the HVAC demand is the greatest. We see that with transactive control, the HVAC power is mostly capped under the peak demand limit. Moreover, the zone temperatures in the occupied hours (06:00–18:00) are strictly regulated within the pre-specified temperature band (19 °C–23 °C). Additionally, temperature deviations are small on average, suggesting additional peak demand shaving potential.

C. Simulation: Responding to a RTP Signal

We next demonstrate how transactive control of commercial building responds to a RTP signal. The signal in this

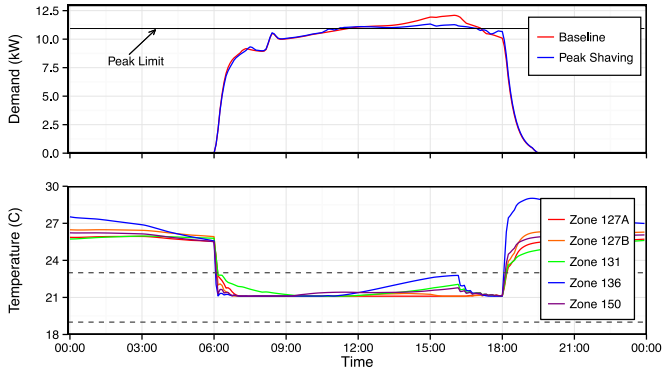

Fig. 6. Comparison of peak demands and zone temperatures with and without transactive control. Note that a constant 21°C temperature set point is used in the baseline case.

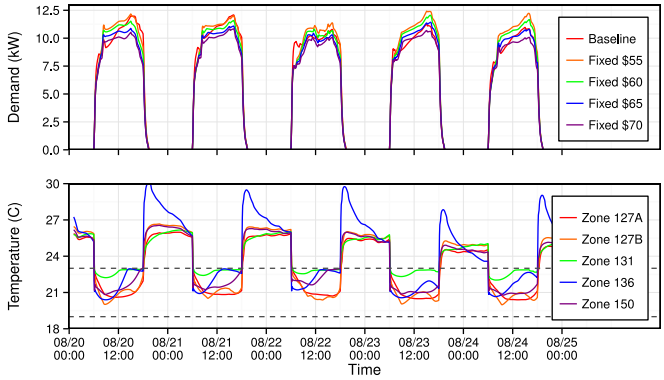

Fig. 8. Power trajectories and zone temperatures of agents competing under fixed prices.

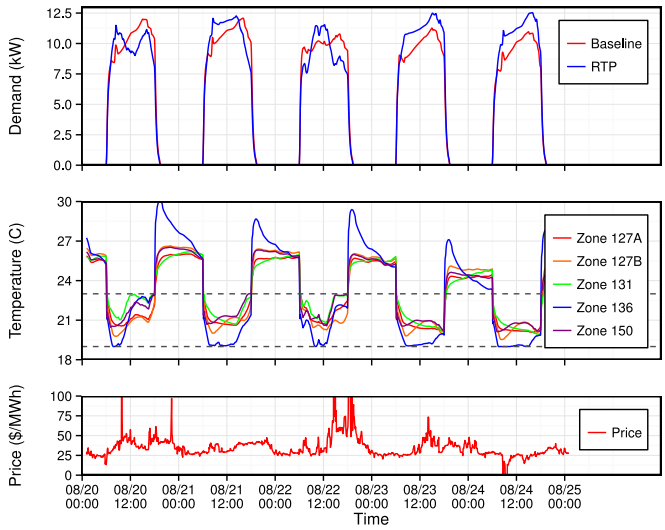

Fig. 7. Transactive control of commercial building HVAC system to respond to a RTP signal.

experiment is a time series of RTPs obtained from the California independent system operator (CAISO) [48]. Zone bid prices are calculated according to Section III-C, using the preceding 24 hours as the averaging period. Market clearing in this case is straightforward: the local electricity market clears at the CAISO real time electricity price, and zone thermostats adjust their temperature set points accordingly. We assume that the RTP at the power network node is independent of building load, i.e., the building demand is a negligible fraction of the total demand at the pricing node and has little impact on the settling price. Fig. 7 shows the impact of RTP on the building power demand and zone temperatures. We observe that the zone temperatures in the occupied hours are strictly regulated within the pre-specified temperature band. Moreover, when electricity price is high, indoor temperatures increase and building power demand reduces; when price is low, indoor temperatures decrease and building power demand increases. This behavior is consistent from day to day for the whole considered week, demonstrating that the transactive market mechanism is capable of shaping building demand according to a dynamic price. We comment that although price-based DR is not our focus, our transactive control scheme is compatible with its implementation.

D. Simulation: Strategic Energy Conservation

The final experiment investigates the market behavior of zone agents when a fixed electricity price is supplied to the local electricity market. In this case, the electricity MCP is equal to this fixed price. As a result, total cooling available is also fixed, although aggregate demand varies from time step to time step due to the changing cooling needs of individual zones. In principle, a fixed price results in an equitable distribution of the available cooling when bidding strategies are the same, as each zone receives an amount of cooling proportional to its need. By selecting an appropriate electricity price, this behavior may be used to encourage lower energy consumption, without penalizing any given zone; zones still receive an amount in proportion to their need, scaled by the cooling available. We set upper and lower bid prices as described in Section IV-B, run the experiment for several fixed prices, and compare the total HVAC energy consumption. HVAC power trajectories shown in Fig. 8 indicate that the higher the price, and therefore the lower the available cooling, the lower the energy consumption. While this is an intuitive result, it is not arrived at by simply increasing all zone set points by a fixed amount. Temperature trajectories illustrate that zones adjust set points at different rates—resulting from different cooling demands—demonstrating a sharing of the responsibility to reduce aggregate demand, facilitated by the market mechanism.

E. Summary and Discussion

Summarized in Table I are impacts of the three incentive signals on building peak demand, energy consumption, and temperature deviation. Peak load reduction is calculated on a daily basis as a percentage of baseline peak load on the same day. Energy consumption is presented as a total percentage change from the baseline, and temperature deviation is measured by the average temperature difference from the nominal 21 °C set point. Note that in the peak load shaving case, baseline demand

TABLE I
IMPACTS OF THE THREE INCENTIVE SIGNALS ON BUILDING PEAK LOAD, ENERGY CONSUMPTION, AND TEMPERATURE DEVIATION

		Peak Load (%)			Energy	Temp.
		Mean	Min	Max	(%)	(°C)
Peak Load Shaving		−6.2	−6.3	−6.1	−1.5	0.17
Responding to RTP		5.8	−4.2	14.2	3.1	−0.03
Fixed Price	$55	5.6	−0.6	11.4	4.7	−0.07
	$60	1.1	−4.2	6.9	1.0	0.30
	$65	−4.2	−9.3	1.4	−3.1	0.61
	$70	−8.5	−12.3	−5.1	−7.1	0.85

exceeds the limit on only the first two days, so calculations do not include the remainder of the week.

We see in the peak load shaving case (see Fig. 6) that baseline peak demand occurs at roughly 15:00. With transactive control, demand cleared in the market remains entirely below the imposed limit. However, due to the model mismatch between our reduced-order models and EnergyPlus model, we observe a slight excursion above this limit. Nevertheless, transactive control is able to reduce peak demand and save energy by raising zone temperatures by only a small amount on average. The systematic quantification of peak load shaving potential w.r.t. temperature deviation is an interesting future research.

In contrast, the case of responding to RTP shows reduced zone temperatures, and increased energy consumption and peak demand on most days. This is because the prices on days four and five look very low compared to those seen in the previous days, which causes agents to bid much higher for air than they would otherwise (refer to the zone bidding strategy described in Section III-C), driving temperature set points lower, and ultimately consuming more cooling energy. This is consistent with findings from [29] and highlights the importance of bidding strategy on system behavior.

In addition to reducing energy consumption, fixed price cases suggest that significant peak load reduction may result. In general, a fixed price tends to flatten demand compared to the baseline, shifting consumption to the morning hours, effectively precooling zones prior to the afternoon peak. This is reflected in temperature profiles in Fig. 8 which show decreased zone temperatures early in the day. It should be noted that selecting the "correct" price that results in energy saving and peak reduction is not obvious, and likely different for each day or season. This is an area of further exploration, and suggests that with a fairly simple market mechanism, buildings could achieve strategic energy conservation, while reducing peak demand, without an external incentive signal.

V. CONCLUSIONS AND FUTURE WORK

We proposed a novel transactive control approach for commercial building HVAC systems to provide DR to the grid. We have presented the system modeling and identification using SEB measurement data. Additionally, a transactive market mechanism was proposed to coordinate different HVAC components to collectively achieve a global objective—DR. We also set up a simulation environment using the BCVTB, calibrated SEB EnergyPlus model, and Python implementation of the transactive market mechanism. Case studies of peak load shaving, responding to a RTP signal, and letting zone agents compete under a fixed price were conducted, and we showed that the proposed transactive control approach was very effective at peak shaving, load shifting, and strategic conservation.

There are many directions for future research. We are currently implementing the proposed transactive market mechanism using VOLTTRON [49], an agent-based distributed sensing and control platform developed at PNNL, on the SEB, and evaluating its performance in field tests. In the future, we will study a multi-period market mechanism, and compare it with the current single-period transactive approach. Moreover, our building-to-grid research has mainly focused on the building side. In the future, we will study how to integrate the transactive market with the electricity wholesale and retail markets, and quantify the potential and economic benefit of transactive building control to both the building owner and the utility/system operator. Another interesting future research is study of incentive compatibility of the transactive mechanism, i.e., how to design a mechanism to ensure agents bid truthfully.

ACKNOWLEDGMENT

The authors greatly acknowledge Viraj Srivastava, Jacob Hansen, Guopeng Liu, Atefe Makhmalbaf, and Siddharth Goyal for their contributions to calibrating HVAC system models, developing market mechanism, constructing EnergyPlus model, and setting up simulation environment, as well as the anonymous reviewers for their constructive comments.

APPENDIX

Proof of Theorem 1: The proof follows similar line of attack as of [31], [50], [51]. We first look at the Karush–Kuhn–Tucker (KKT) optimality conditions for the individual utility maximization problem (4),

$$\begin{cases} \nabla V^i(Q^{i,*}) + \nu_1^{i,*} - \nu_2^{i,*} - p_a^{i,*} = 0 & \forall\, i, \\ Q_-^i - Q^{i,*} \le 0 & \forall\, i, \\ \nu_1^{i,*} \ge 0 & \forall\, i, \\ \nu_1^{i,*}(Q_-^i - Q^{i,*}) = 0 & \forall\, i, \\ Q^{i,*} - Q_+^i \le 0 & \forall\, i, \\ \nu_2^{i,*} \ge 0 & \forall\, i, \\ \nu_2^{i,*}(Q^{i,*} - Q_+^i) = 0 & \forall\, i, \end{cases} \tag{6}$$

where $\nabla V^i(Q^{i,*})$ is derivative of V^i at $Q^{i,*}$, and $Q^{i,*}$ is the optimal solution of (4). We next define λ^* as $p_a^{i,*} = (\lambda^* + \nabla C(Q^*))\nabla g_i(Q^{1,*}, \cdots, Q^{n,*})$. It can be shown that if $g\big(Q^{1,*}, \cdots, Q^{n,*}\big) - D < 0$, we have $p_a^{i,*} = \nabla C(Q^*)\nabla g_i(Q^{1,*}, \cdots, Q^{n,*})$, which implies $\lambda^* = 0$. Otherwise, we have $p_a^{i,*} = \bar{P}\nabla g_i(Q^{1,*}, \cdots, Q^{n,*}) \ge \nabla C(Q^*)\nabla g_i(Q^{1,*}, \cdots, Q^{n,*})$, which shows that $\lambda^* \ge 0$. In conclusion, we can show that the above conditions (6) together with the optimal air and electricity prices are equivalent to the

KKT conditions of the SWM problem (5),

$$\begin{cases} \nabla V^i(Q^{i,*}) + \nu_1^{i,*} - \nu_2^{i,*} - \lambda^*(g\big(Q^{1,*},\cdots,Q^{n,*}\big) - D) \\ \qquad -(\lambda^* + \nabla C(Q^*))\nabla g_i(Q^{1,*},\cdots,Q^{n,*}) = 0 & \forall\, i, \\ Q_-^i - Q^{i,*} \le 0 & \forall\, i, \\ \nu_1^{i,*} \ge 0 & \forall\, i, \\ \nu_1^{i,*}(Q_-^i - Q^{i,*}) = 0 & \forall\, i, \\ Q^{i,*} - Q_+^i \le 0 & \forall\, i, \\ \nu_2^{i,*} \ge 0 & \forall\, i, \\ \nu_2^{i,*}(Q^{i,*} - Q_+^i) = 0 & \forall\, i, \\ g\big(Q^{1,*},\cdots,Q^{n,*}\big) - D \le 0 \\ \lambda^* \ge 0, \\ \lambda^*(g\big(Q^{1,*},\cdots,Q^{n,*}\big) - D) = 0 \end{cases}$$

where λ^* is the Lagrange variable associated with the peak demand limit constraint. This completes the proof. ■

REFERENCES

[1] United States Department of Energy, "Benefits of demand response in electricity markets and recommendations for achieving them," Feb. 2006.

[2] Buildings energy data book. [Online]. Available: http://buildingsdatabook.eren.doe.gov/default.aspx

[3] Energy Information Administration, United States Department of Energy, "Commercial buildings energy consumption survey: Overview of commercial buildings," Dec. 2012.

[4] H. Hao, T. Middelkoop, P. Barooah, and S. Meyn, "How demand response from commercial buildings will provide the regulation needs of the grid," in *Proc. Annu. Allerton Conf. Commun., Control, Comput.*, 2012, pp. 1908–1913.

[5] F. Oldewurtel, A. Ulbig, M. Morari, and G. Andersson, "Building control and storage management with dynamic tariffs for shaping demand response," in *Proc. IEEE PES Int. Conf. Exhib. Innovative Smart Grid Technol.*, 2011, pp. 1–8.

[6] H. Hao, Y. Lin, A. Kowli, P. Barooah, and S. Meyn, "Ancillary service to the grid through control of fans in commercial building HVAC systems," *IEEE Trans. Smart Grid*, vol. 5, no. 4, pp. 2066–2074, Jul. 2014.

[7] J. Hughes, A. Domínguez-García, and K. Poolla, "Virtual battery models for load flexibility from commercial buildings," in *Proc. Hawaii Int. Conf. Syst. Sci.*, Kauai, HI, USA, 2015, pp. 2627–2635.

[8] S. Wang, X. Xue, and C. Yan, "Building power demand response methods toward smart grid," *HVAC&R Res.*, vol. 20, no. 6, pp. 665–687, 2014.

[9] D. Li, S. K. Jayaweera, O. Lavrova, and R. Jordan, "Load management for price-based demand response scheduling—A block scheduling model," in *Proc. Int. Conf. Renew. Energies Power Quality*, Las Palmas de Gran Canaria, Spain, 2011.

[10] North American Electric Reliability Corporation, "Data collection for demand-side management for quantifying its influence on reliability results and recommendations," Dec. 2007.

[11] M. Roozbehani, M. A. Dahleh, and S. K. Mitter, "Volatility of power grids under real-time pricing," *IEEE Trans. Power Syst.*, vol. 27, no. 4, pp. 1926–1940, Nov. 2012.

[12] A. M. Kosek, G. T. Costanzo, H. W. Bindner, and O. Gehrke, "An overview of demand side management control schemes for buildings in smart grids," in *Proc. IEEE Int. Conf. Smart Energy Grid Eng.*, 2013, pp. 1–9.

[13] E. Koch and A. M. Piette, "Direct versus facility centric load control for automated demand," presented at the Grid-Interop Forum, Denver, CO, USA, 2009.

[14] N. O'Connell, P. Pinson, H. Madsen, and M. O'Malley, "Benefits and challenges of electrical demand response: A critical review," *Renew. Sustain. Energy Rev.*, vol. 39, pp. 686–699, 2014.

[15] T. W. Haring, J. L. Mathieu, and G. Andersson, "Comparing centralized and decentralized contract design enabling direct load control for reserves," *IEEE Trans. Power Syst.*, vol. 31, no. 3, pp. 2044–2054, May 2016.

[16] D. Callaway and I. Hiskens, "Achieving controllability of electric loads," *Proc. IEEE*, vol. 99, no. 1, pp. 184–199, Jan. 2011.

[17] K. Margellos and S. Oren, "Capacity controlled demand side management: A stochastic pricing analysis," *IEEE Trans. Power Syst.*, vol. 31, no. 1, pp. 706–717, Jan. 2016.

[18] R. Li, Q. Wu, and S. S. Oren, "Distribution locational marginal pricing for optimal electric vehicle charging management," *IEEE Trans. Power Syst.*, vol. 29, no. 1, pp. 203–211, Jan. 2014.

[19] J. L. Mathieu, S. Koch, and D. S. Callaway, "State estimation and control of electric loads to manage real-time energy imbalance," *IEEE Trans. Power Syst.*, vol. 28, no. 1, pp. 430–440, Feb. 2013.

[20] J. L. Mathieu, M. Kamgarpour, J. Lygeros, G. Andersson, and D. S. Callaway, "Arbitraging intraday wholesale energy market prices with aggregations of thermostatic loads," *IEEE Trans. Power Syst.*, vol. 30, no. 2, pp. 763–772, Mar. 2015.

[21] S. P. Meyn, P. Barooah, A. Busic, Y. Chen, and J. Ehren, "Ancillary service to the grid using intelligent deferrable loads," *IEEE Trans. Automat. Control*, vol. 60, no. 11, pp. 2847–2862, Nov. 2015.

[22] S. Meyn, P. Barooah, A. Busic, and J. Ehren, "Ancillary service to the grid from deferrable loads: the case for intelligent pool pumps in Florida," in *Proc. IEEE Conf. Decision Control*, 2013, pp. 6946–6953.

[23] L. Chen, N. Li, S. H. Low, and J. C. Doyle, "Two market models for demand response in power networks," in *Proc. IEEE SmartGridComm*, 2010, pp. 397–402.

[24] N. Li, L. Chen, and S. H. Low, "Optimal demand response based on utility maximization in power networks," in *Proc. IEEE Power & Energy Soc. General Meeting*, 2011, pp. 1–8.

[25] H. Hao, B. M. Sanandaji, K. Poolla, and T. L. Vincent, "Aggregate flexibility of thermostatically controlled loads," *IEEE Trans. Power Syst.*, vol. 30, no. 1, pp. 189–198, Jan. 2015.

[26] H. Hao and W. Chen, "Characterizing flexibility of an aggregation of deferrable loads," in *Proc. IEEE Conf. Decision Control*, 2014, pp. 4059–4064.

[27] S. Somasundaram, R. Pratt, B. Akyol *et al.*, "Reference guide for a transaction-based building controls framework," Pacific Northwest Nat. Lab., Richland, WA, USA, Tech. Rep. PNNL-23302, Apr. 2014.

[28] D. Hammerstrom, R. Ambrosio, J. Brous *et al.*, "Pacific northwest gridwise testbed demonstration projects," Pacific Northwest Nat. Lab., Richland, WA, USA, Tech. Rep. PNNL-17167, 2007.

[29] S. E. Widergren, K. Subbarao, J. C. Fuller *et al.*, "AEP Ohio gridsmart demonstration project real-time pricing demonstration analysis," Pacific Northwest Nat. Lab., Richland, WA, USA, Tech. Rep. PNNL-23192, 2014.

[30] S. Katipamula, D. P. Chassin, D. D. Hatley *et al.*, "Transactive controls: Market-based gridwise controls for building systems," Pacific Northwest Nat. Lab., Richland, WA, USA, Tech. Rep. PNNL-17632, 2006.

[31] S. Li, W. Zhang, J. Lian, and K. Kalsi, "Market-based coordination of thermostatically controlled loads. Part I: A mechanism design formulation," *IEEE Trans. Power Syst.*, vol. 31, no. 2, pp. 1170–1178, Mar. 2016.

[32] B. A. Huberman and S. H. Clearwater, "A multi-agent system for controlling building environments," in *Proc. Int. Conf. Multiagent Syst.*, 1995, pp. 171–176.

[33] M. Wetter, "Co-simulation of building energy and control systems with the building controls virtual test bed," *J. Building Perform. Simul.*, vol. 4, no. 3, pp. 185–203, 2011.

[34] D. B. Crawley, L. K. Lawrie, F. C. Winkelmann *et al.*, "Energyplus: Creating a new-generation building energy simulation program," *Energy Buildings*, vol. 33, no. 4, pp. 319–331, 2001.

[35] Y. Ma and F. Borrelli, "Fast stochastic predictive control for building temperature regulation," in *Proc. Amer. Control Conf.*, Jun. 2012, pp. 3075–3080.

[36] N. Radhakrishnan, Y. Su, R. Su, and K. Poolla, "Token based scheduling of HVAC services in commercial buildings," in *Proc. Amer. Control Conf.*, 2015, pp. 262–269.

[37] ASHRAE, "The ASHRAE handbook HVAC systems and equipment (SI Edition)," 2008.

[38] Department of Energy, "Energyplus engineering reference," 2010. [Online]. Available: http://www.openadr.org/assets/June2014/18_final_tc-te-oadr

[39] Y.-W. Wang, W.-J. Cai, Y.-C. Soh, S.-J. Li, L. Lu, and L. Xie, "A simplified modeling of cooling coils for control and optimization of HVAC systems," *Energy Convers. Manage.*, vol. 45, no. 18, pp. 2915–2930, 2004.

[40] Y. Yao, Z. Lian, and Z. Hou, "Thermal analysis of cooling coils based on a dynamic model," *Appl. Thermal Eng.*, vol. 24, no. 7, pp. 1037–1050, 2004.

[41] L. Lu, W. Cai, L. Xie, S. Li, and Y. C. Soh, "HVAC system optimization—In-building section," *Energy and Buildings*, vol. 37, no. 1, pp. 11–22, 2005.

[42] R Core Team, *R: A Language and Environment for Statistical Computing*, R Foundation for Statistical Computing, Vienna, Austria, 2014. [Online]. Available: http://www.R-project.org/
[43] H. Liu, Y. Shen, Z. B. Zabinsky, C.-C. Liu, A. Courts, and S.-K. Joo, "Social welfare maximization in transmission enhancement considering network congestion," *IEEE Trans. Power Syst.*, vol. 23, no. 3, pp. 1105–1114, Aug. 2008.
[44] H. Niu, R. Baldick, and G. Zhu, "Supply function equilibrium bidding strategies with fixed forward contracts," *IEEE Trans. Power Syst.*, vol. 20, no. 4, pp. 1859–1867, Nov. 2005.
[45] L. Xu and R. Baldick, "Transmission-constrained residual demand derivative in electricity markets," *IEEE Trans. Power Syst.*, vol. 22, no. 4, pp. 1563–1573, Nov. 2007.
[46] Y. Xu, N. Li, and S. H. Low, "Demand response with capacity constrained supply function bidding," *IEEE Trans. Power Syst.*, vol. 31, no. 2, pp. 1377–1394, Mar. 2016.
[47] R. Johari and J. N. Tsitsiklis, "Parameterized supply function bidding: Equilibrium and efficiency," *Oper. Res.*, vol. 59, no. 5, pp. 1079–1089, 2011.
[48] California ISO open access same-time information system (OASIS). [Online]. Available: http://oasis.caiso.com
[49] Pacific Northwest National Laboratory, "VOLTTRON: An agent execution platform," Oct. 2014. [Online]. Available: http://transactionalnetwork.pnnl.gov/volttron.stm
[50] J. M. Arroyo and F. D. Galiana, "Energy and reserve pricing in security and network-constrained electricity markets," *IEEE Trans. Power Syst.*, vol. 20, no. 2, pp. 634–643, May 2005
[51] S. Boyd and L. Vandenberghe, *Convex Optimization*. Cambridge, U.K.: Cambridge Univ. Press, 2004.

He Hao received the B.S. degree in mechanical engineering and automation from Northeastern University, Shenyang, China, in 2006, the M.S. degree in mechanical engineering from Zhejiang University, Hangzhou, China, in 2008, and the Ph.D. degree in mechanical engineering from the University of Florida, Gainesville, FL, USA, in 2012. Between January 2013 to July 2014, he was a Postdoctoral Research Fellow with the Department of Electrical Engineering and Computer Science, University of California, Berkeley, CA, USA. He is currently a Staff Scientist in the Electricity Infrastructure and Buildings Division at Pacific Northwest National Laboratory, Richland, WA, USA. His research interests include power system, smart buildings, distributed control and optimization, and large-scale complex systems.

Charles D. Corbin received the B.S. degree from Cornell University in 1999 and the M.S. and Ph.D. degrees from the University of Colorado in 2009 and 2014, respectively. He is a Researcher at the Pacific Northwest National Laboratory in the Advanced Building Controls Team, working in both Building Energy Systems and Electricity Infrastructure groups. His research interests include integration of buildings and renewable energy with power system operations, advanced building controls and diagnostics, machine learning, and complex systems.

Karanjit Kalsi received the M.Eng. degree from the University of Sheffield, Sheffield, U.K., in 2006, and the Ph.D. degree in electrical and computer engineering from Purdue University, West Lafayette, IN, USA, in 2010. He is currently a Power Systems Research Engineer at the Pacific Northwest National Laboratory, Richland, WA, USA.

Robert G. Pratt received the B.S. degree in ocean engineering from Florida Atlantic University and the M.S. degree in mechanical engineering from Colorado State University. He has been a Scientist at Pacific Northwest National Laboratory since 1985. He is one of the early thought leaders behind the smart grid, focused on an information-rich future for the power grid. He manages Pacific Northwest National Laboratory's Smart Grid R&D program activities for the U.S. Department of Energy. He leads a team studying communications architecture, advanced control technology, and simulation of the combined engineering and economic aspects of the future grid, including the effect of plug-in hybrid electric vehicles.